

REANALYSIS OF THE GAS-COOLED FAST REACTOR EXPERIMENTS AT THE ZERO POWER FACILITY PROTEUS – SPECTRAL INDICES

Gregory Perret, Rajesh M. Pattupara
Paul Scherrer Institute
5232 Villigen, Switzerland
gregory.perret@psi.ch; rmpattupara@gmail.com

Gaëtan Girardin, Rakesh Chawla*
Ecole Polytechnique Fédérale de Lausanne
1015 Lausanne, Switzerland
gaetan.girardin@epfl.ch; rakesh.chawla@epfl.ch

ABSTRACT

The gas-cooled fast reactor (GCFR) concept was investigated experimentally in the PROTEUS zero power facility at the Paul Scherrer Institute during the 1970's. The experimental program was aimed at neutronics studies specific to the GCFR and at the validation of nuclear data in fast spectra. A significant part of the program used thorium oxide and thorium metal fuel either distributed quasi-homogeneously in the reference PuO₂/UO₂ lattice or introduced in the form of radial and axial blanket zones. Experimental results obtained at the time are still of high relevance in view of the current consideration of the Gas-cooled Fast Reactor (GFR) as a Generation-IV nuclear system, as also of the renewed interest in the thorium cycle. In this context, some of the experiments have been modeled with modern Monte Carlo codes to better account for the complex PROTEUS whole-reactor geometry and to allow validating recent continuous neutron cross-section libraries. As a first step, the MCNPX model was used to test the JEFF-3.1, JEFF-3.1.1, ENDF/B-VII.0 and JENDL-3.3 libraries against spectral indices, notably involving fission and capture of ²³²Th and ²³⁷Np, measured in GFR-like lattices.

Key Words: Gas-cooled Fast Reactor, Spectral Indices, Research Reactors, PROTEUS, MCNP.

1. INTRODUCTION

The Gas-cooled Fast Reactor (GFR) is one of the concepts proposed in the framework of the Generation-IV (GEN-IV) initiative to develop safe, sustainable, reliable, proliferation-resistant and economic nuclear energy systems. This reactor has a fast spectrum that can maximize the usage of uranium resources thanks to its potential for a high breeding gain, and it can also be used for high temperature applications such as hydrogen production [1]. Although the Sodium-cooled Fast Reactor is seen today as the most promising concept in GEN-IV, the GFR remains one of the main alternative systems. In this context, the neutronic and thermal-hydraulic properties of the GFR have been recently analyzed within the Nuclear Energy and Safety division of the Paul Scherrer Institute (PSI), using the in-house code system FAST [2, 3, 4, 5].

* Co-affiliation: Paul Scherrer Institute, 5232 Villigen, Switzerland.

Interest in gas-cooled fast reactors (GCFRs), however, is not new. Already in the 1970's, the neutronics of early GCFR designs was investigated experimentally in the PROTEUS zero power reactor at the Paul Scherrer Institute (PSI) in Switzerland [6]. The experimental program comprised a large set of PROTEUS configurations to validate lattice and core calculation methods and associated nuclear data libraries. Most of the experiments were related to PuO₂/UO₂ fuelled GCFRs, i.e. to the commonly applied ²³⁸U/²³⁹Pu fuel cycle. However, several core configurations were dedicated to nuclear data validation for the alternative ²³²Th/²³³U fuel cycle. For instance, fuel lattices with thorium oxide and thorium metal fuel rods allowed investigating the self-shielding of thorium capture cross-sections in fast spectra. Thorium rods were also arranged to form axial and radial blankets to study the interface with PuO₂/UO₂, which is of particular interest for breeding ²³³U in fast reactors. Radial and axial reaction rate traverses, as well as spectral indices, were measured to characterize the breeding ratio, power distribution, neutron spectrum, etc.

Experimental results were compared in the 1970's with 1D and 2D deterministic predictions obtained using the SN-1D/DIFF-1D and DIFF-2D code systems, in conjunction with ENDF/B-IV and FGL5 cross-sections prepared by the GGC-4 and MURLAB cell codes. The agreement between calculated and experimental results was overall quite satisfactory. In 2006, the renewed interest in gas-cooled fast reactors prompted a reassessment of the past experimental results on the basis of modern codes and nuclear data libraries [7]. These studies were performed at the cell level using correction factors calculated in the 1970's to account for differences in the spectra between the PROTEUS test zone and the cell model. In the frame of a recent Master's thesis [8], we developed a new 3D model of the full GCFR-PROTEUS reactor, using the Monte Carlo code MCNPX, to compare an extended set of the GCFR-PROTEUS measurements to predictions by modern codes and libraries.

As a first step, the new GCFR-PROTEUS whole-reactor model is used in this paper to predict spectral indices in the center of the test zone and to compare them with values calculated in a critical single zone lattice, as well as to the values measured in PROTEUS. The first comparison serves to shed light on how representative the PROTEUS experiments are of a large GCFR. The second comparison allows us to validate the cross-sections of the traditional plutonium and uranium isotopes but also those for ²³⁷Np and ²³²Th capture and fission, ²³³U fission, and (n,2n) reaction in ²³²Th. Calculated predictions are based on the modern continuous energy libraries JEFF-3.1, JEFF-3.1.1, ENDF/B-VII.0 and JENDL-3.3.

The following section briefly reviews the GCFR-PROTEUS program, with emphasis on the two experimental configurations considered currently. The calculation models and the representativity of the PROTEUS experiments are discussed in Section 3, while the comparison of the calculated spectral indices with measured values is presented in Section 4. The final section provides the conclusions.

2. GCFR EXPERIMENTS AT PROTEUS

In this section, we briefly describe the arrangement of the PROTEUS reactor and the main studies performed during the GCFR experiments. We detail the two lattice configurations used in

this paper to validate the calculated spectral indices. We finally shortly recall how the spectral indices were measured and what their uncertainties were.

2.1. Experiments and Core Configurations

PROTEUS is a zero-power reactor featuring a cylindrical central cavity that is driven critical by a surrounding graphite region fueled with 5 w% UO_2 fuel pins. The central cavity can be filled with different fuel arrangements to study different reactor concepts. In the GCFR experiments, the central cavity was loaded with a D_2O zone fueled with 5 w% UO_2 fuel pins, a buffer region containing metallic natural uranium rods in air and a central test zone filled with a GCFR-representative fuel lattice (see Fig. 1). This multi-zone arrangement has the advantage of reducing, by a factor of ~ 10 , the amount of plutonium required to obtain a critical mock-up representative of the fast reactor under study. The buffer region modifies the incident driver flux and plays a crucial role in ensuring that the PROTEUS central neutron spectrum is close to that of a single zone reactor.

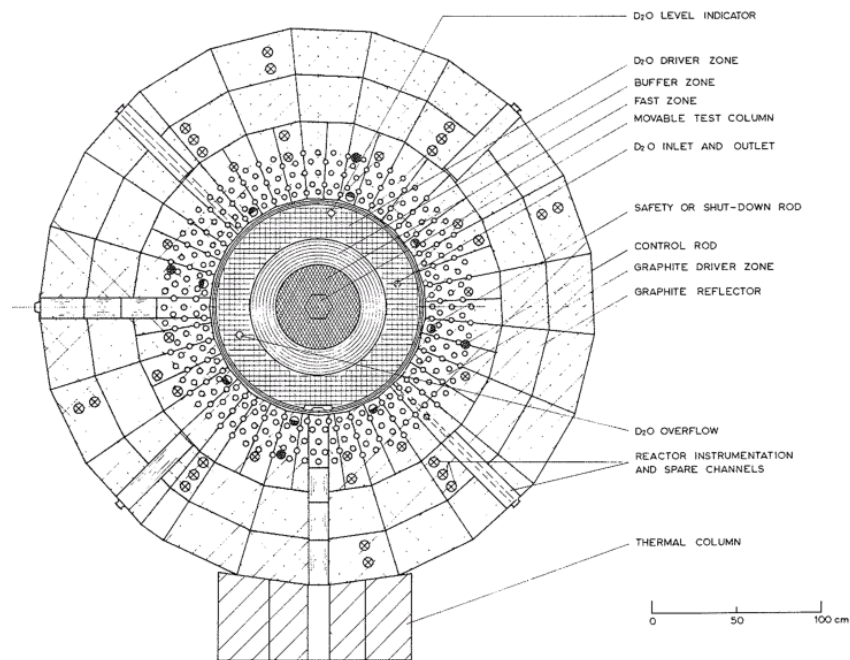


Figure 1. PROTEUS horizontal section during the GCFR experiments

In the GCFR experiments, about 20 different core configurations were studied from 1972 to 1979. The reference configuration featured in the central test zone a regular hexagonal lattice (1 cm pitch) of PuO_2/UO_2 fuel rods. The fuel contained 15 w% plutonium, of which $\sim 80\%$ was fissile, and was clad in stainless steel. The fuel pellets had a diameter of 6.7 mm and a density of 10.6 g/cm^3 and provided an active length of $\sim 0.83 \text{ m}$ sandwiched between a top and a bottom blanket of depleted uranium ($0.42 \text{ w}\% \text{ }^{235}\text{U}$, 10.5 g/cm^3) to make up a total fuel length of 1.4 m.

In the first part of the measurement campaign, the reference PuO₂/UO₂ core configuration was altered to simulate steam/water entry, effects of a sub-assembly stainless steel wall, B₄C control rods and radial depleted uranium blankets. A large steel reflector (0.6 m thick) was also added on top of the central zone to benchmark iron cross-section data. The second part of the campaign was dedicated to the study of thorium nuclear data in a GCFR spectrum. For this purpose, the reference PuO₂/UO₂ test zone was modified to include, in turn, ThO₂ and thorium metal fuel rods, distributed either quasi-homogenously in the lattice, or introduced in the form of radial and axial blanket zones.

In this paper we focus on two of the GCFR-PROTEUS configuration, i.e. the reference configuration described above and a mixed test lattice configuration, in which 1/3 of the PuO₂/UO₂ rods were uniformly replaced with ThO₂ rods. In the latter lattice, the thorium oxide fuel was in the form of sintered particles with a density of 9.9 g/cm³ and a diameter of ~400 μm. The particles were packed into 18/8-steel clad “cigars” to provide an effective ThO₂ fuel density of 6.08 g/cm³. Axially, both the PuO₂/UO₂ and the ThO₂ fuel were bounded at both ends by the same length of depleted UO₂.

2.2. Measurement Techniques for the Spectral Indices

Reaction rate ratios were measured using metal foils (²³⁸U, ²³²Th), aluminum-alloyed fission foils (²³⁹Pu, ²³⁵U, ²³³U) and thin deposits on aluminum backing (²³⁷Np). The number of heavy atoms in the aluminum-alloyed foils could not be determined accurately; therefore, spectral indices relative to fissions in ²³⁹Pu required the use of additional calibrated ²³⁹Pu deposits in back-to-back fission chambers. These fission chambers were inserted into a core cavity (CC), ~20 cm above the reactor center, and into the thermal column (TC) located in the graphite reflector of the reactor (see Fig. 1). This allowed making two types of spectral indices measurements: absolute and relative to the thermal column (a.k.a. thermal comparison technique) [9].

The measurement procedures are best illustrated by describing the set-up of an irradiation to measure the ²³²Th capture to ²³⁹Pu fission ratio (C2/F9) and the ²³²Th fission to ²³⁹Pu fission ratio (F2/F9). For these measurements, ²³⁹Pu and ²³²Th foils were inserted between fuel pellets at the core center, and a fission chamber with a calibrated ²³⁹Pu deposit – as well as ²³²Th and ²³⁹Pu foils – were inserted into the core cavity; similarly loaded fission chamber and foils were placed in the thermal column. The C2/F9 index could then be determined absolutely and by thermal comparison. For the absolute measurement, C2 was deduced from an absolute measurement of the 312 keV gamma-ray line emitted by ²³³Pa, and F9 was determined from the ratio of the activities of the foils irradiated in the core center and in the core cavity and from the absolute ²³⁹Pu rate measured using the fission chamber in the core cavity. For the measurement by thermal comparison, C2/F9 was obtained as: $C2_{RC} / F9_{RC} = (C2_{RC} / C2_{TC}) (F9_{TC} / F9_{CC}) (F9_{CC} / F9_{RC}) (C2_{TC} / F9_{TC})$ where RC, TC and CC denote reactor center, thermal column and core cavity, respectively. The last term is the same index in a thermal spectrum and is known from the thermal cross-sections for ²³²Th capture and ²³⁹Pu fission; the other terms are measured. The thermal comparisons technique cannot, of course, be used for threshold reactions like fission in ²³²Th, and F2/F9 was determined only by absolute measurement. Similar techniques were used to measure captures and fissions in ²³⁸U and ²³⁷Np. For the (n,2n)-to-capture ratio in ²³²Th, a single thorium foil irradiated at the center of the test lattice was measured, removing the need to determine the number of ²³²Th atoms.

Measurements with foils are sensitive to self-shielding effects, and the thickness of the foils is a crucial parameter, especially when measuring an infinite-dilution reaction rate (e.g. C2 in a PuO_2/UO_2 fuel). Self-shielding was carefully accounted for by measuring reaction rates with foils of different thickness. Among the errors considered in the absolute measurements, the statistical counting errors (1σ) were in the range 0.1-1%, and the errors associated with gamma self-absorption were about 0.5% for capture in ^{232}Th and ^{238}U , and 1.5% for $^{232}\text{Th}(n,2n)$. The higher uncertainty for the (n,2n) reaction comes from the low energy (25.6 keV) of the measured ^{231}Th gamma-ray. For the thermal comparison measurements the self-absorption error becomes negligible but 1-2% errors on the thermal cross-section values need to be considered. Using C and F as abbreviations for capture and fission, and 2, 3, 5, 7, 8 and 9 for ^{232}Th , ^{233}U , ^{235}U , ^{237}Np , ^{238}U and ^{239}Pu , the total uncertainty on the measured spectral indices were 1.1-1.3% for C8/F9, F8/F9, F5/F9, F3/F9 and C2/F9, 1.8-2% for F7/F9 and F2/F9, and 2.3-2.5% for C7/F9 and (n,2n)2/C2.

3. CALCULATION MODELS AND REPRESENTATIVITY OF THE EXPERIMENTS

3.1. Cell Models

Cell models of the reference regular PuO_2/UO_2 lattice and the mixed $\text{PuO}_2/\text{UO}_2 - \text{ThO}_2$ lattice were set-up with MCNPX-2.5 [10]. Horizontal sections are shown in Fig. 2. The radial boundaries are reflective and the height is adjusted to reach criticality. Critical heights for the regular and mixed lattices are about 80 and 165 cm, respectively. Flux and spectral indices as well as their energy distributions are tallied in the central 10 cm of the PuO_2/UO_2 and ThO_2 fuel, where the foils measurements were performed. Calculations have been carried out with the ENDF/B-VII.0 [11], JEFF-3.1 [12], JEFF-3.1.1 [13] and JENDL-3.3 [14] data libraries.

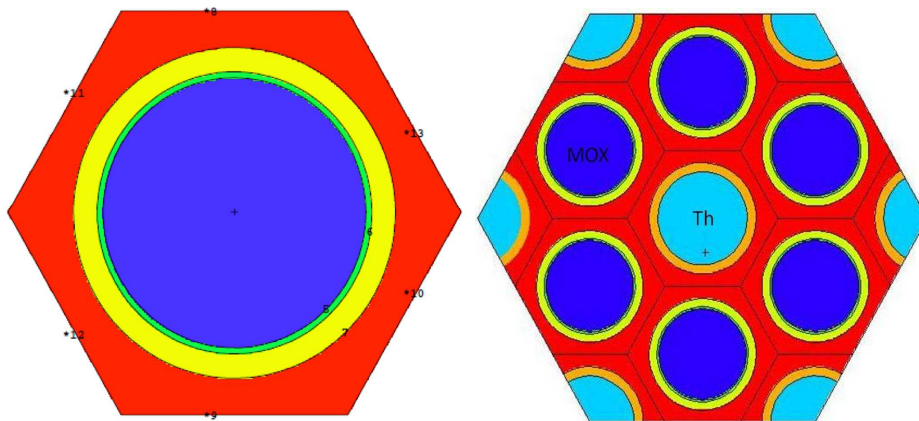


Figure 2. Horizontal sections of the cell models for the regular PuO_2/UO_2 (left) and the mixed $\text{PuO}_2/\text{UO}_2 - \text{ThO}_2$ (right) lattices

The neutron flux spectrum in the PuO_2/UO_2 fuel of the regular lattice is shown in Fig. 3 for three of the libraries (with 2σ error bars indicated). The median energy is about 185 keV and the flux below 100 eV is negligible in all cases. ENDF/B-VII.0 and JENDL-3.3 are seen to agree very

well, whereas the predicted flux with JEFF-3.1 (and JEFF-3.1.1) is slightly higher between 110 keV and 820 keV. Running additional calculations showed that this effect is readily due to the ^{238}U cross-sections, most probably because of differences in the inelastic scattering. For the mixed lattice, slightly higher lower-energy fluxes were obtained in the PuO_2/UO_2 and ThO_2 rods (median energy ~ 180 keV), but the results stayed qualitatively unchanged.

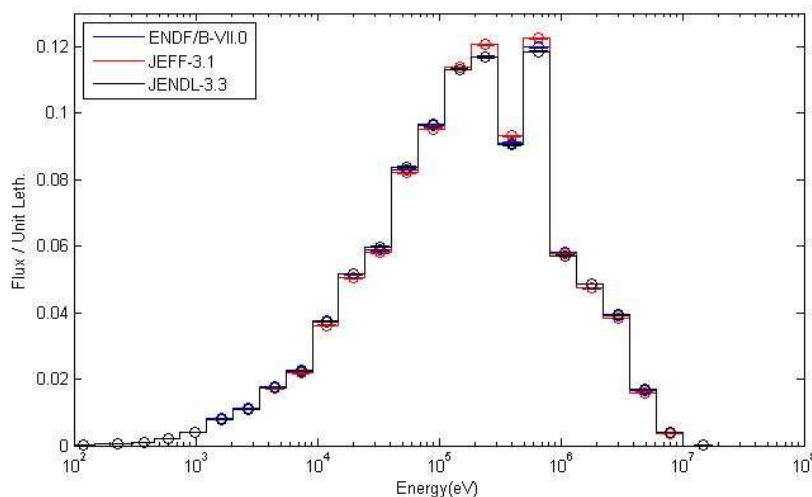


Figure 3. Flux spectra in the PuO_2/UO_2 fuel for the reference configuration calculated with ENDF/B-VII.0, JEFF-3.1 and JENDL-3.3 libraries

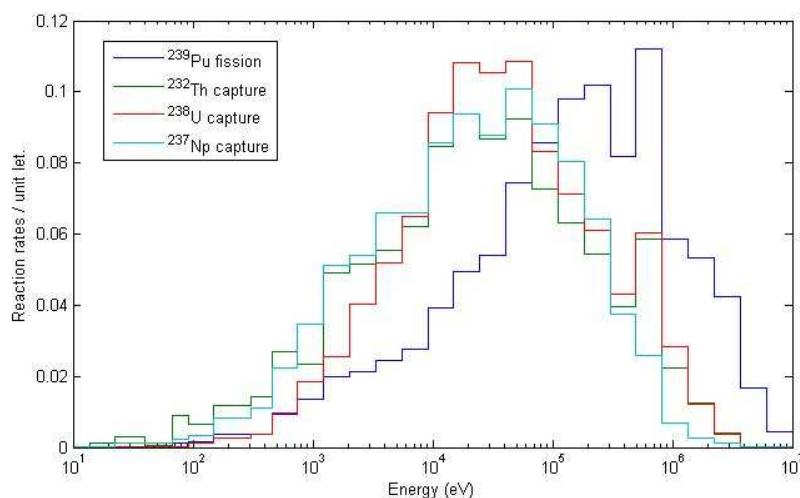


Figure 4. Energy distributions for ^{239}Pu fission and ^{238}U , ^{237}Np and ^{232}Th capture rates in the PuO_2/UO_2 fuel of the reference lattice, calculated with MCNPX and ENDF/B-VII.0

Fig. 4 shows the energy decomposition for the ^{239}Pu fission, ^{238}U capture, ^{237}Np capture and ^{232}Th capture rates in the reference lattice using the ENDF/B-VII.0 data. Captures in ^{232}Th and ^{237}Np are seen to be significantly more sensitive to lower-energy neutrons than fissions in ^{239}Pu or even captures in ^{238}U . For example, less than 0.3% of the ^{239}Pu fissions and ^{238}U captures occur below 150 eV, whereas the corresponding fractions for captures in ^{237}Np and ^{232}Th are about 1% and 1.7%, respectively. The latter two reactions are therefore expected to be more

sensitive to any low energy neutrons coming from the driver regions of PROTEUS that have not been converted in the buffer (see Section 3.3).

3.2. Whole-Reactor Models

The development of the whole-reactor model of PROTEUS, as used for the GCFR experiments has been a painstaking task because of the complex geometry of the critical facility and the many differences between the GCFR experiments and the LWR-PROTEUS program for which a model was developed previously [15]. Horizontal and vertical sections of the whole-reactor model are shown in Fig. 5 for the case of the reference PuO_2/UO_2 core lattice to illustrate this point. The effort invested to model the two different test-lattice configurations presented in this paper will be built upon in the future, when modeling the other configurations of the PROTEUS-GCFR program.

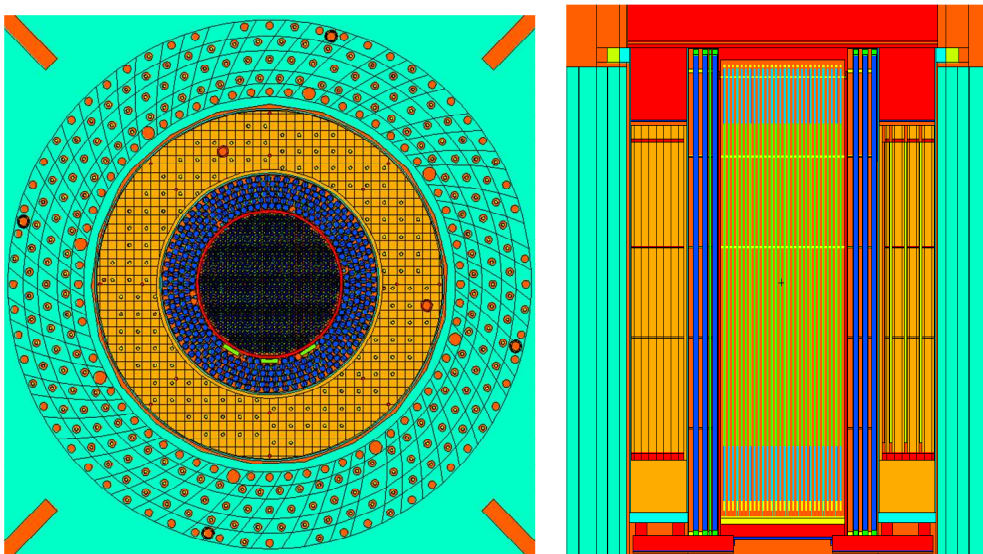


Figure 5. Horizontal and vertical section of the PROTEUS whole-reactor MCNPX model

For the results presented in this paper, the flux and reaction rates of interest were tallied in the central pins of the test zone in which the spectrum is as close as possible to that in a single zone reactor. Axially, the tallies were limited to 10 cm to prevent any spectral distortion due to the depleted uranium blankets. Calculations were run with ENDF/B-VII.0, JEFF-3.1, JEFF-3.1.1 and JENDL-3.3, and the differences in k_{eff} values were less than 200 pcm. Calculations were run with 250 million neutrons for JENDL-3.3 and JEFF-3.1.1. Calculations with JEFF-3.1 and ENDF/B-VII.0 were run longer for an improved accuracy on the spectral index involving (n,2n) reactions in thorium (see Section 4).

3.3. Representativity of the PROTEUS Experiments

As mentioned in the introduction, one of the key advantages of the GCFR-PROTEUS experiments has been to limit the amount of plutonium required to achieve a fast spectrum representative of a GCFR. This can be tested qualitatively by comparing the flux spectrum of the cell and whole-reactor models. Fig. 6 shows such a comparison for the reference lattice using the ENDF/B-VII.0 library (with 2σ error bars indicated). The figure is shown on a log-linear scale, and the low energy region is zoomed in the insert shown on a log-log scale. The whole-reactor

model flux is seen to exhibit a lower median energy. However, the fraction of neutrons below 1 keV changes only slightly from 0.4% to 0.6% when using the whole-reactor instead of the cell model; in both cases, the flux below 100 eV is less than 0.1%. Therefore, the spectrum at the center of the PROTEUS test zone indeed well represents the GCFR spectrum.

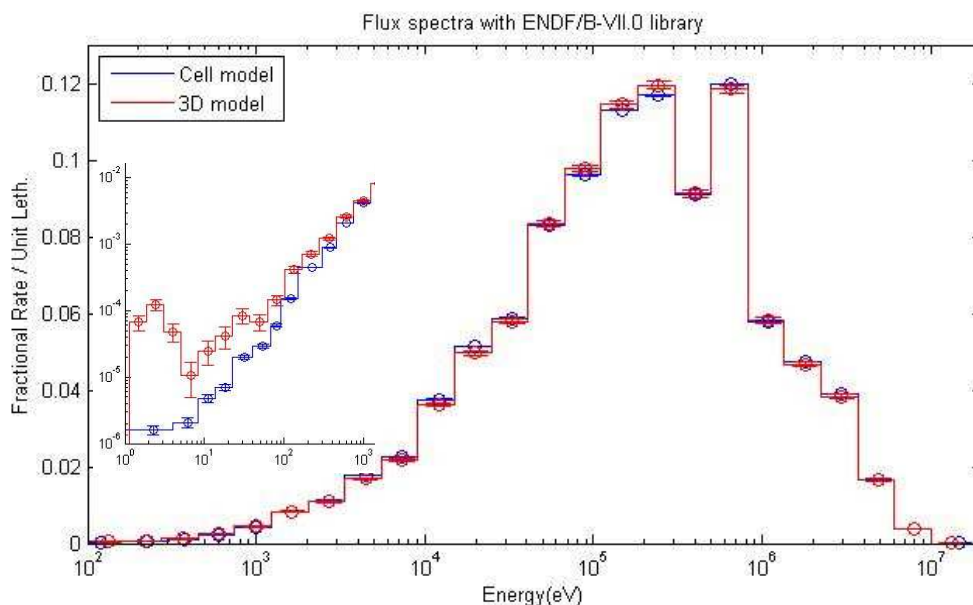


Figure 6. Flux spectra in the central PuO₂/UO₂ fuel pin of the whole-reactor model and from the cell calculation

It is also interesting to compute the ratio of the spectral indices calculated in the two models, as they directly show the relevance of measuring spectral indices in PROTEUS to validate cross-sections in GCFR spectra. These ratios – or correction factors – are summarized in Table I for the four libraries mentioned previously, as well as for the FGL5 library, which was used in conjunction with deterministic codes in the original analysis of the experimental results [9]. In Table I and in the rest of the paper C and F stand for capture and fission and 2, 3, 5, 7, 8 and 9 for ²³²Th, ²³³U, ²³⁵U, ²³⁷Np, ²³⁸U and ²³⁹Pu, respectively.

Table I. Correction factors for spectral indices in the reference lattice with their 1σ uncertainties

Spectral Index	FGL5*	ENDF/B-VII.0	JEFF-3.1	JENDL-3.3	JEFF-3.1.1
C8/F9	0.994 (0.5%)	0.988 (0.2%)	0.990 (0.2%)	0.988 (0.3%)	0.987 (0.3%)
F8/F9	0.974 (0.5%)	0.978 (0.2%)	0.974 (0.3%)	0.979 (0.4%)	0.973 (0.4%)
F5/F9	1.004 (0.5%)	1.004 (0.2%)	1.004 (0.2%)	1.007 (0.3%)	1.003 (0.3%)
C2/F9	1.002 (0.5%)	1.028 (0.5%)	1.027 (0.7%)	1.035 (1%)	1.038 (0.9%)
F2/F9	0.979 (0.5%)	0.978 (0.3%)	0.976 (0.4%)	0.980 (0.5%)	0.974 (0.5%)
F3/F9	1.027 (0.5%)	1.026 (0.2%)	1.024 (0.2%)	1.027 (0.3%)	1.026 (0.3%)
(n,2n)2/C2	0.975 (0.5%)	0.965 (1.5%)	0.979 (2.1%)	0.927 (2.9%)	0.918 (2.9%)
C7/F9	1.020 (1%)	1.033 (0.2%)	1.035 (0.4%)	1.035 (0.5%)	1.038 (0.5%)
F7/F9	0.975 (1%)	0.981 (0.2%)	0.977 (0.3%)	0.981 (0.3%)	0.979 (0.3%)

*Cross-section library from U.K. used in the 70's with deterministic calculations

Although the indicated (1σ) Monte Carlo uncertainties on the C2/F9 and (n,2n)2/C2 spectral indices are high, we can draw several conclusions. All correction factors stand within 5% of unity, except for (n,2n)2/C2 as calculated using JENDL-3.3 and JEFF-3.1.1, for which the statistical uncertainty is too high to draw clear conclusions. Very good consistency is observed for the different data libraries used with MCNPX, as the average dispersion for each spectral index is compatible with the standard deviation on each calculation. Results predicted by the Monte Carlo model do not differ significantly from the results obtained with deterministic codes and the FGL5 data library. Only the C2/F9 index does not agree within 2σ .

All in all, we have shown that the spectrum in the center of the PROTEUS test zone is representative of a GCFR and that the correction factors calculated with MCNPX compare favorably with the originally reported deterministic values. In the next section, the spectral indices predicted with the MCNPX whole-reactor model are compared directly with the experimental results in both the regular PuO₂/UO₂ and the mixed PuO₂/UO₂ - ThO₂ lattices.

4. COMPARISON OF SPECTRAL INDICES PREDICTION WITH EXPERIMENT

A large set of spectral indices was measured in the reference lattice using foils and fission chambers (see Section 2.2). Measurements are compared to code predictions in Table II in the form of calculation-to-experiment ratio with their 1σ uncertainty. Results obtained with the deterministic codes and the FGL5 library during the 1970's are reproduced for completeness [9, 16].

Table II. Calculation-to-experiment ratios for spectral indices in the reference lattice with their 1σ uncertainties (differences greater than 2σ are shown bold).

Spectral Index	FGL5	ENDF/B-VII.0	JEFF-3.1	JENDL-3.3	JEFF-3.1.1
C8/F9	0.984 (1.1%)	0.995 (1.2%)	0.993 (1.2%)	0.993 (1.2%)	0.991 (1.2%)
F8/F9	1.045 (1.3%)	1.009 (1.4%)	0.992 (1.4%)	1.032 (1.4%)	0.992 (1.4%)
F5/F9	-	1.012 (1.5%)	1.012 (1.5%)	1.009 (1.5%)	1.011 (1.5%)
C2/F9	0.972 (1.3%)	1.015 (1.4%)	0.985 (1.5%)	0.931 (1.6%)	0.994 (1.6%)
F2/F9	0.888 (2.0%)	0.913 (2.1%)	0.965 (2.1%)	0.996 (2.1%)	0.965 (2.1%)
F3/F9	0.990 (1.3%)	0.987 (1.4%)	0.992 (1.4%)	0.990 (1.4%)	0.995 (1.4%)
(n,2n)2/C2	1.019 (2.5%)	1.084 (2.9%)	1.112 (3.2%)	1.026 (3.8%)	1.051 (3.8%)
C7/F9	1.102 (2.3%)	1.003 (2.4%)	0.951 (2.4%)	0.953 (2.4%)	0.966 (2.4%)
F7/F9	0.983 (1.8%)	1.003 (1.9%)	1.006 (1.9%)	1.006 (1.9%)	0.969 (1.9%)

MCNPX whole-reactor model with modern libraries yields very good predictions for fission in ²³⁵U and ²³³U as compared to fission in ²³⁹Pu. For fissions in ²³⁸U, ²³⁷Np and ²³²Th, only reactions above the 0.5 to 1 MeV thresholds are significant in this spectrum. Good agreement is seen for the ²³⁷Np fission reaction, which has the lowest threshold. Only a small trend can be seen in JEFF-3.1.1 where the ²³⁷Np fission cross-section has been re-assessed [13]. Fission in ²³⁸U is well predicted by JEFF-3.1, JEFF-3.1.1 and ENDF/B-VII.0, and slightly overestimated by JENDL-3.3. ²³²Th fissions, on the other hand, are underestimated by as much as $8.7\pm 2.1\%$ by ENDF/B-VII.0, the agreement for the other three libraries being within 2σ . The underestimation

is mainly due to differences in the cross-sections. This is surprising considering that the ^{232}Th fission cross-sections in ENDF/B-VII.0 were re-evaluated recently using the latest measurements performed at the n_TOF and GELINA facilities [17].

^{238}U captures are well predicted by all libraries in MCNPX. ^{232}Th captures are somewhat underestimated using JENDL-3.3. The re-evaluated cross-sections in JEFF-3.1/3.1.1 and ENDF/B-VII.0 lead to better agreement with the experiments. ^{237}Np captures are slightly underestimated with JENDL-3.3 and JEFF-3.1. The new evaluation of the capture cross-section of ^{237}Np in JEFF-3.1.1 is mainly in the thermal and resonance range. In the fast GCFR-PROTEUS spectrum, the new cross-section slightly improves the prediction by about 1%. Note that the uncertainties on the measured C2/F9 and C7/F9 spectral indices are 1.3% and 2.3%, respectively*. Longer MCNPX runs would therefore not change the picture significantly.

For the (n,2n)2/C2 spectral index, the uncertainty on the MCNPX whole-reactor model prediction is not negligible as compared to the uncertainty on the experimental value (2.5%). This is why the whole-reactor model with the two reference libraries ENDF/B-VII.0 and JEFF-3.1 were run with more particles. Because of the time required to run this calculation, the process was not currently extended to the other libraries. (n,2n)2/C2 spectral index is significantly overestimated ($\sim 10 \pm 3\%$) using ENDF/B-VII.0 or JEFF-3.1, whereas the agreement for JENDL-3.3 and JEFF-3.1.1 is reasonable. Interestingly the thorium cross-sections are the same in JEFF-3.1 and 3.1.1 and the values of the calculated C2/F9 index are the same (within $1 \pm 1\%$). The suggested change in the (n,2n)2/C2 predictions ($5.3 \pm 3.4\%$) could thus be ascribed to differences in the flux above 6.5 MeV.

The spectral indices involving ^{232}Th and ^{238}U reactions were also measured in the mixed $\text{PuO}_2/\text{UO}_2 - \text{ThO}_2$ lattice. In this case, ^{232}Th foils were inserted into the ThO_2 rods in order to investigate the self-shielding effect for ^{232}Th capture. Past and present predictions are compared to the experiments in Table III in the form of calculation-to-experiment values. Results obtained in the regular PuO_2/UO_2 lattice are also duplicated in Table III to ease comparison.

Table III. Calculation-to-experiment ratios for spectral indices in the reference PuO_2/UO_2 and mixed $\text{PuO}_2/\text{UO}_2 - \text{ThO}_2$ lattices

Spectral Index	PuO ₂ /UO ₂ lattice		Mixed PuO ₂ /UO ₂ - ThO ₂ lattice	
	FGL5	JEFF-3.1	FGL5	JEFF-3.1
C8/F9	0.984	0.993 (1.2%)	0.979	0.993 (1.8%)
F8/F9	1.045	0.992 (1.4%)	1.046	0.973 (1.8%)
C2/F9	0.972	0.985 (1.5%)	1.041	0.996 (1.8%)
F2/F9	0.888	0.965 (2.1%)	0.887	0.945 (1.8%)
(n,2n)2/C2	1.019	1.112 (3.2%)	1.079	1.157 (7.2%)

As expected, the slight underestimation of fission in ^{232}Th is confirmed in the mixed lattice, but the results are still a large improvement on the values calculated in the past. Similarly, the uncertainty on the (n,2n)2/C2 index remains high, and it is hard to draw a clear conclusion. Future longer calculations, especially for the mixed lattice, could shed light on the possible over-

* As can be seen in the FGL5 column of Table II.

prediction observed with JEFF-3.1. Finally, the C2/F9 index is in perfect agreement in the ThO₂ rods of the mixed lattice. The self-shielding effect is thus well predicted by the code.

5. CONCLUSIONS

A large experimental program, dedicated to the study of gas-cooled fast reactors (GCFR), was carried out at the PROTEUS zero-power reactor in the 1970's. Spectral indices, reaction rate distributions and reactivity effects were measured to characterize the breeding ratio, power distribution, neutron spectrum, etc. Several modifications to the hexagonal PuO₂/UO₂ reference lattice (15 w% Pu) were carried out to simulate the impact of steam/water entry, large reflector zones, absorber rods, sub-assembly stainless steel wall, etc. A large subset of experiments was also dedicated to the use of thorium in GCFRs and focused on validating ²³²Th cross-sections and code predictions for axial and radial thorium blanket regions.

Given the renewed interest for the use of thorium, as well as the fact that the GFR is a concept supported by the GEN-IV initiative, the PROTEUS experiments are still of high value today. Their re-analysis with modern tools can thus be quite beneficial. In this frame, we set-up a generic 3D whole-reactor MCNPX model of the PROTEUS reactor as it was deployed in the GCFR experiments. As a first step, we used the 3D model to (i) check whether the spectrum in the center of the PROTEUS test zone is indeed representative of a GCFR, and (ii) to validate the recent ENDF/B-VII.0, JEFF-3.1/3.1.1 and JENDL-3.3 libraries against a wide range of spectral index measurements.

The spectrum at the center of the test zone has been confirmed to be very close to that of a large single zone GCFR (1-3%). As regards the spectral indices measured in the reference regular PuO₂/UO₂ lattice, a good overall agreement has been found. The ratio of ²³²Th fission to ²³⁹Pu fission (F2/F9), however, is under-predicted by 8.7±2.1% using ENDF/B-VII.0. JENDL-3.3 underestimates the ratio of ²³²Th capture to ²³⁹Pu fission (C2/F9) by 6.9±1.6% and overestimates the ²³⁸U-to-²³⁹Pu fission ratio (F8/F9) by 3.2±1.4%. As regards the (n,2n) reactions in ²³²Th, although the uncertainties remain high, both ENDF/B-VII.0 and JEFF-3.1 seem to overestimate the reaction by about 10±3%. Finally, JEFF-3.1 and JENDL-3.3 tend to underestimate the ²³⁷Np capture rate, the agreement being slightly better with JEFF-3.1.1.

Spectral index measurements in a mixed PuO₂/UO₂ - ThO₂ lattice have also been analyzed in this paper. Very good agreement has been obtained for the ²³²Th capture rate measured in the ThO₂ fuel pin, indicating that the self-shielding effect is well predicted with MCNPX and JEFF-3.1. In the future, predictions of spectral indices measured in thorium metal fuel (with a higher density of 11.3 g/cm³) could confirm this effect further.

Over and above the other GCFR-PROTEUS configurations in which spectral indices were measured, several other types of investigations were carried out at the time, e.g. reaction rate traverses across thorium/MOX interfaces. These could help validate codes and data libraries for gas-cooled fast reactors and thorium usage in a broader context. In closing, we remain convinced that GCFR-PROTEUS experiments – despite their age – represent a large source of carefully measured experimental data whose re-analysis can benefit the nuclear community today.

REFERENCES

1. R. Stainsby et al., “Gas Cooled Fast Reactor Research and Development in the European Union”, *Science and Technology of Nuclear Installations*, **2009**, (2009).
2. K. Mikityuk, “FAST code system: review of recent developments and near-future plans,” *Proceeding of the 17th International Conference on Nuclear Energy ICONE17*, Brussels, Belgium, July 12-16, (2009).
3. G. Girardin et al., “Development and characterization of the control assembly system for the large 2400 MWth Generation IV GFR”, *Annals of Nuclear Energy*, **35**, pp.2206-2218 (2008).
4. P. Petkevich et al., “Development and benchmarking of a mechanical model for GFR plate-type fuel,” *Annals of Nuclear Energy*, **36**, pp.1262-1269 (2009).
5. A. Epiney et al., “Heavy gas injection in the GEN-IV GFR to improve decay heat removal under depressurized conditions,” *Proceeding of NURETH 2009*, Kanazawa, Japan, (2009).
6. R. Richmond, “Measurement of the Physics Properties of Gas-Cooled Fast Reactors in the Zero Energy Reactor PROTEUS and Analysis of the Results,” Eidg. Institut für Reaktorforshung – EIR Report 478.
7. G. Girardin, “Comparative analysis of the reference GCFR-PROTEUS MOX lattice with MCNPX-2.5e and ERANOS-2.0 in conjunction with modern nuclear data libraries,” *Proceeding of Physor '06*, Vancouver, BC, Canada, Sept. 10-14, (2006)
8. R. M. Pattupara, “Monte Carlo Analysis of PROTEUS GCFR Experiments”, EPFL Master Thesis (2011).
9. R. Chawla et al., “Fast Reactor Experiments with Thorium at the PROTEUS Facility,” Eidg. Institut für Reaktorforshung – EIR Report 444.
10. D. B. Pelowitz, “MCNPX User’s Manual Version 2.5.0,” Los Alamos National Laboratory Report LA-CP-05-0369.
11. M.B. Chadwick et al., “ENDF/B-VII.0: Next Generation Evaluated Nuclear Data Library for Nuclear Science and Technology,” *Nuclear Data Sheets*, **107**, pp. 2931-3060 (2006).
12. A. Koning et al., “The JEFF-3.1 Nuclear Data Library,” in JEFF Report 21, NEA No. 6190, ISBN 92-64-02314-3 (2006).
13. A. Santamarina et al., “The JEFF-3.1.1 Nuclear Data Library,” in JEFF Report 22, NEA No. 6807, ISBN 978-92-64-99074-6 (2009).
14. K. Shibata et al., “Japanese Evaluated Nuclear Data Library Version 3 Revision-3: JENDL-3.3,” *J. Nucl. Sci. Technol.*, **39**, pp. 1125-1136 (2002).
15. O. P. Joneja et al., “Validation of an MCNP4B whole-reactor model for LWR-PROTEUS using ENDF/B-V, ENDF/B-VI and JEFF-2.2 cross-section libraries,” *Annals of Nuclear Energy*, **28**, pp. 701-713 (2001).
16. R. Chawla et al., “Integral testing of ^{237}Np cross-sections in GCFR spectra,” *Annals of Nuclear Energy*, **6**, pp. 585-589 (1979).
17. R. Capote et al., “Evaluated Nuclear Data for Nuclides within the Thorium-Uranium Fuel Cycle,” IAEA Report 1435, (2010).